International Journal of Hematology
https://doi.org/10.1007/s12185-019-02782-z

ORIGINAL ARTICLE

Evaluation of clinical severity in patients with type 2N von Willebrand disease using microchip-based flow-chamber system

Yuto Nakajima[1] · Keiji Nogami[1] · Koji Yada[1,2] · Takeshi Kawamura[1] · Kenichi Ogiwara[1] · Shoko Furukawa[1,3] · Naruto Shimonishi[1] · Masahiro Takeyama[1] · Midori Shima[1]

Received: 30 August 2019 / Revised: 8 November 2019 / Accepted: 12 November 2019

Abstract

Type 2N von Willebrand disease (VWD) is characterized by impaired factor VIII (FVIII) binding to von Willebrand factor (VWF). Type 2N VWD patients generally exhibit mild bleeding tendency, but some exhibit a more severe hemorrhagic pattern. An assay for assessing hemostatic potential and predict clinical severity could significantly improve clinical management in these patients. We examined the relationship between bleeding score (BS) and the potential for thrombus formation in whole blood from type 2N VWD patients with various BS using rotational thromboelastometry (ROTEM) and microchip flow-chamber system (T-TAS®). Collagen-coated PL-chips, or thromboplastin- and collagen-coated AR-chips, were utilized in the T-TAS to assess platelet thrombus formation at high shear flow, or fibrin-rich platelet thrombus formation at low shear flow, respectively. Neither ROTEM nor the T-TAS using PL-chips reflected the BS. The AR-chip parameters in the T-TAS, however, were highly sensitive to different BS levels among these patients, despite similar FVIII/VWF-related measurements including FVIII/VWF binding. Additionally, the results with AR-chip assay were restored to normal after infusions of FVIII/VWF concentrates in the most severe patients. The data indicate that T-TAS using AR-chips may be a useful assay for predicting clinical severity and assessing therapeutic efficiency in type 2N VWD patients.

Keywords Microchip flow-chamber system · Type 2N von willebrand disease · Von willebrand factor · Bleeding score · Clinical severity

Introduction

von Willebrand disease (VWD) is a common inherited mucocutaneous bleeding disorder resulting from defective or deficient von Willebrand factor (VWF). The diagnosis of VWD is commonly characterized by conventional laboratory analyses of VWF antigen (VWF:Ag), VWF ristocetin cofactor activity (VWF:RCo) and factor VIII activity (FVIII:C). On this basis, VWD is categorized into three disease types; partial (type 1) and virtually complete (type 3) quantitative deficiency of VWF, and qualitative VWF defects (type 2) [1]. Type 2 VWD is subdivided into 4 variants (2A, 2B, 2M and 2N) with defined functional abnormalities of VWF. Type 2N VWD is characterized by reduced plasma levels of FVIII and a defect in the FVIII and VWF interaction, resulting in a clinical phenotype resembling mild or moderate hemophilia A [2]. Patients with type 2N VWD usually present a mild bleeding phenotype [3], although investigators in the Netherlands (the WIN study group) [4] demonstrated that the median bleeding score (BS) in patients with this type was 10, and that some patients in this category exhibited more severe clinical symptoms. In addition, the standardized BS assessment using the questionnaire is utilized for evaluating the clinical severity of VWD, but this index does not always correlate with VWF:Ag and/or VWF:RCo levels [5, 6]. The evidence suggests, therefore, that current laboratory assays do not adequately reflect the

An account of this work was presented at the 25th Congress of the International Society on Thrombosis and Haemostasis, 2015, Toronto, Canada.

✉ Keiji Nogami
roc-noga@naramed-u.ac.jp

[1] Department of Pediatrics, Nara Medical University, 840 Shijo-cho, Kashihara 634-8522, Nara, Japan

[2] The Course of Hemophilia Education, Nara Medical University, Kashihara, Nara, Japan

[3] The Course of Thrombosis and Hemostasis Molecular Pathology, Nara Medical University, Kashihara, Nara, Japan

Published online: 18 November 2019

clinical severity in type 2N VWD patients, and that a method to assess hemostatic potential and predict clinical severity could benefit clinical management in these patients.

In this context, the blood flow-based systems have been previously devised to assess comprehensive hemostasis especially related to VWF and platelet function under the shear stress [7, 8].An automated microchip flow-chamber system (T-TAS®, Fujimori Kogyo, Tokyo, Japan), has been recently developed as an easy-to-use system for visualizing platelet thrombus formation (PTF) on surfaces coated with collagen (PL-chips) under the high shear or fibrin-rich PTF on surfaces coated with collagen and tissue factor (AR-chips) under the low shear. This technique could provide novel, useful information for assessing the diagnosis and treatment of VWD [9–11]. Our earlier studies indicated that the analysis using both assays of coated chips might be useful for classifying clinical phenotypes and monitoring the therapeutic effects of desmopressin and FVIII/VWF complex concentrates in VWD [9]. In particular, Nogami et al. [10] demonstrated that the PL-chip assay could effectively assess the clinical severity in type 1 VWD patients. In addition, Ågren et al. reported that the T-TAS could provide valuable data for evaluating the therapeutic effects of FVIII/VWF concentrates in type 3 VWD patients [11]. However, the usefulness of T-TAS in patients with type 2 VWD, caused by dysfunctional VWF on the FVIII binding, remains to be investigated.

The present study was designed, therefore, to investigate whether the T-TAS could define the clinical severity, and monitor the therapeutic effects of FVIII/VWF complex concentrates in patients with type 2N VWD. The relationship between the BS and T-TAS parameters was examined and compared with results from rotational thromboelastometry (ROTEM) using whole blood in these individuals.

Materials and methods

Blood samples

The study was approved by the Medical Research Ethics Committee of Nara Medical University. Blood samples were obtained after informed consent according to the ethical guidelines of the university. Blood samples were taken from 20 healthy volunteers (controls) and 5 patients, previously diagnosed definitely as type 2N VWD in the participated hospitals. Whole blood samples were collected into plastic tubes containing 3.2% sodium citrate at a ratio of 9:1 (Fuso Pharmaceutical Industries, Osaka, Japan) or into tubes containing hirudin (final concentration; f.c. 25 μg mL^{-1}, Roche Diagnostics, Rotkreuz, Switzerland). There were no study subjects that had taken any medication that may have influenced platelet or coagulation function in 2 weeks prior to blood sampling. Platelet poor plasma was separated by centrifugation of the citrated whole blood for 10 min at 2000×*g*. All plasma samples were stored at − 80 °C and thawed at 37 °C immediately prior to subsequent processing of the assays.

Diagnosis of type 2N VWD

The diagnosis for type 2N VWD was based on the standardized criteria using conventional functional assays such as FVIII activity (FVIII:C), VWF:RCo, VWF:Ag and FVIII/VWF-binding assay (VWF:FVIIIB) [12].

Bleeding score (BS) assessment

The clinical severity of hemorrhagic symptoms in type 2N VWD patients was assessed using the questionnaire from Molecular and Clinical Markers for the Diagnosis and Management of Type 1 VWD study (MCMDM-1) [6].

VWD-related laboratory assays

We performed an in-house enzyme-linked immunosorbent assay (ELISA) with polyclonal rabbit anti-human VWF and horseradish peroxidase-conjugated anti-VWF antibodies (Dako, Glostrup, Denmark) to measure VWF:Ag levels, as previously described [13]. We further determined the VWF:RCo and FVIII:C levels by utilizing the standard glass-plate method with formalin-fixed platelets and by a one-stage clotting assay, respectively, as previously described [14, 15].

VWF:FVIIIB was assessed by an ELISA-based binding assay [12]. In brief, anti-VWF monoclonal antibody (NMC-VWF/4 [16]) was immobilized onto microtiter wells overnight at 4 °C. The wells were washed with veronal buffer, followed by blocking with veronal buffer containing 3% bovine serum albumin for 2 h at 37 °C. After washing the wells, 100 μl of serial dilutions of plasma samples were added and incubated overnight at 4 °C. After removal of endogenous FVIII using 0.4 M $CaCl_2$, 100 μl of recombinant FVIII (Advate®; Shire) was added and incubated for 1 h at 37 °C. The wells were washed and bound FVIII was quantified by measuring FVIII:C with the chromogenic assay (COATEST®SP FVIII, Instrumentation Laboratory, Bedford, MA, USA). After measuring, the wells were washed, and immobilized VWF was measured by an ELISA using an anti-human peroxidase-conjugated VWF polyclonal antibody (Haematologic Technologies Inc., Essex Junction, VT, USA). In each experiment, the least square regression line for plasma sample was calculated. The slope of the obtained regression lines reflected the binding capacity of VWF to FVIII.

Gene analyses

Genomic DNA was extracted and isolated from leukocytes in the citrated whole blood samples obtained from the patients using QIAGEN QIAquick PCR Purification Kit (Qiagen, Venlo, Netherland) [17]. The coding region of VWF gene (*VWF*) was amplified by the polymerase chain reaction (PCR) with the specific primer sets [18, 19]. The PCR products were applied in a capillary sequencer 3500 genetic analyzer (Applied Biosystems, Foster, CA, USA). The sequence was determined and compared with the consensus *VWF* sequences obtained from the VWF variant database (https://vwf.group.shef.ac.uk). The VWF mutations were explored in the hot spots including exons 4, 9, 17–21 and 24–27 of *VWF* and analyzed by the commercial data collection software in the present study.

T-TAS analysis

The T-TAS assay (Fujimori Kogyo) was performed with minor modifications, based on the protocol recommended [9, 20]. Two modes of microchip, collagen-coated (PL-chip) and collagen/thromboplastin-coated (AR-chip) were used for the respective analysis of PTF (platelet thrombus formation) and fibrin-rich PTF. Whole blood samples were pushed into the capillary path of the microchip with an injection pump. The formation of thrombus within the capillaries resulted in occlusion and was analyzed by monitoring flow-pressure changes. This system also provided video microscope of individual samples for further evaluation of the process of thrombus formation.

Collagen-coated (PL-chip) Hirudin-anticoagulated whole blood (350 µL) was loaded into the collagen-coated capillary under a constant flow rate of 12 µL min^{-1}, corresponding to a shear rate of 1000 s^{-1}. To analyze the PTF, the time taken to reach the increase in flow pressure to 10 kPa (T_{10}) from baseline because of the partial occlusion of the capillaries, and AUC_{10} (area under curve for 10 min) were analyzed.

Collagen/thromboplastin-coated (AR-chip) Citrated whole blood (416 µL) was preincubated with corn trypsin inhibitor (14 µL; f.c. 30 µg mL^{-1}) for 10 min at 37 °C, and mixed with 0.2 M $CaCl_2$ (30 µL). The re-calcified blood sample was perfused through the collagen/thromboplastin-coated capillary under a constant flow rate of 8 µL min^{-1}, corresponding to a shear rate of 240 s^{-1}. The parameters T_{10} and AUC_{30} (AUC for 30 min) were analyzed to assess fibrin-rich thrombus formation inside the AR-chip.

Rotational thromboelastometry (ROTEM)

ROTEM was performed using a Whole Blood Hemostasis Analyzer® (Pentapharm, Munich, Germany). Citrated whole blood samples were incubated for 30 min at room temperature. Immediately before initiation of the measurement, $CaCl_2$ (20 µL, f.c. 12.5 mM) was added to the blood samples (280 µL). We evaluated clot formation utilizing four parameters: the clotting time (CT; the period until reaching a 2-mm amplitude) and clot formation time (CFT; the period until reaching a 20-mm amplitude). The α-angle and maximum clot firmness (MCF) were defined as the angle between the baseline and a tangent to the clotting curve through the 2 mm time point and as the maximum amplitude observed, respectively.

Data analysis

Data analysis was performed using Microsoft Excel software. T-TAS and ROTEM parameters that differed from the mean by ± 2 standard deviations were defined as abnormal.

Patients' profiles

Table 1 summarizes the VWF-related laboratory findings and VWF gene mutations from the 5 patients with type 2N VWD (3 males and 2 females). The BS of these patients varied from 0 to 27. All patients had a FVIII:C/VWF:Ag ratio of < 0.2 and a severely decreased VWF:FVIIIB (<10%). Patients 2, 3 and 4 were identified as having the heterozygous *p*.R816W mutation (patient 2 and 3 were siblings). Patient 1 had a compound heterozygous *p*.T791M mutation in combination with a *p*.R365X mutation previously reported in type 3 VWD [21]. Patient 1 was identified as case 4 in our previous study [9]. Informed consent for genetic analyses for the patient 5 was not available.

Results

Relationship of ROTEM parameters with BS in type 2N VWD

We initially analyzed whole blood samples from all patients with type 2N VWD by ROTEM, and examined the relationship between the patients' BS and ROTEM parameters. In this study, we used NATEM mode, because this mode could evaluate under the neutral trigger condition on initiation of coagulation [22]. Figure 1 shows representative thromboelastograms for each case, together with parameter data. The mean CT, CT + CFT, α-angle and MCF obtained in 20 normal controls were 938 ± 128 s, 1273 ± 217 s, 41.1 ± 7.0° and 43.1 ± 4.6 mm, respectively. ROTEM analysis demonstrated that all patients had significantly prolonged CT and CT + CFT (>2SD). The CT and CT + CFT in patient 3 were the most prolonged even though his BS was 0. In contrast, patient 1 had the highest BS 27, but the CT and CT + CFT were only mildly prolonged. In addition, α-angle and MCF

Table 1 Characteristic profiles of type 2N VWD patients

	Case 1	Case 2	Case 3	Case 4	Case 5	Reference range
Sex	F	F	M	M	M	
Age (years old)	56	25	15	56	58	
Hemoglobin (g/dL)	8.7	13.3	14.2	16.2	14.3	11.6–14.8
WBC ($\times 10^3/\mu L$)	4.8	6.0	4.1	7.9	8.6	3.3–8.6
Platelet ($\times 10^3/\mu L$)	219	273	249	207	333	158–348
PT-INR	1.06	1.00	1.04	0.88	0.97	0.9–1.1
APTT (sec)	50.1	55	59	50.2	52.9	22–32
Fibrinogen (mg/dL)	284	261	234	296	473	200–400
VWF:Ag (IU/dL)	45	79	52	35	59	50–155
VWF:RCo (IU/dL)	32	79	53	32	46	60–170
FVIII:C (IU/dL)	5.0	8.0	4.0	5.3	4.0	60–150
VWF:FVIIIB (% of control)	< 5	< 5	< 5	6.8	< 5	70–110
Bleeding score[#]	27	2	0	5	7	
VWF mutation	p.T791M/p.R365X	p.R816W hetero	p.R816W hetero	p.R816W hetero	ND	

ND not done, *VWF:FVIIIB* FVIII/VWF-binding activity

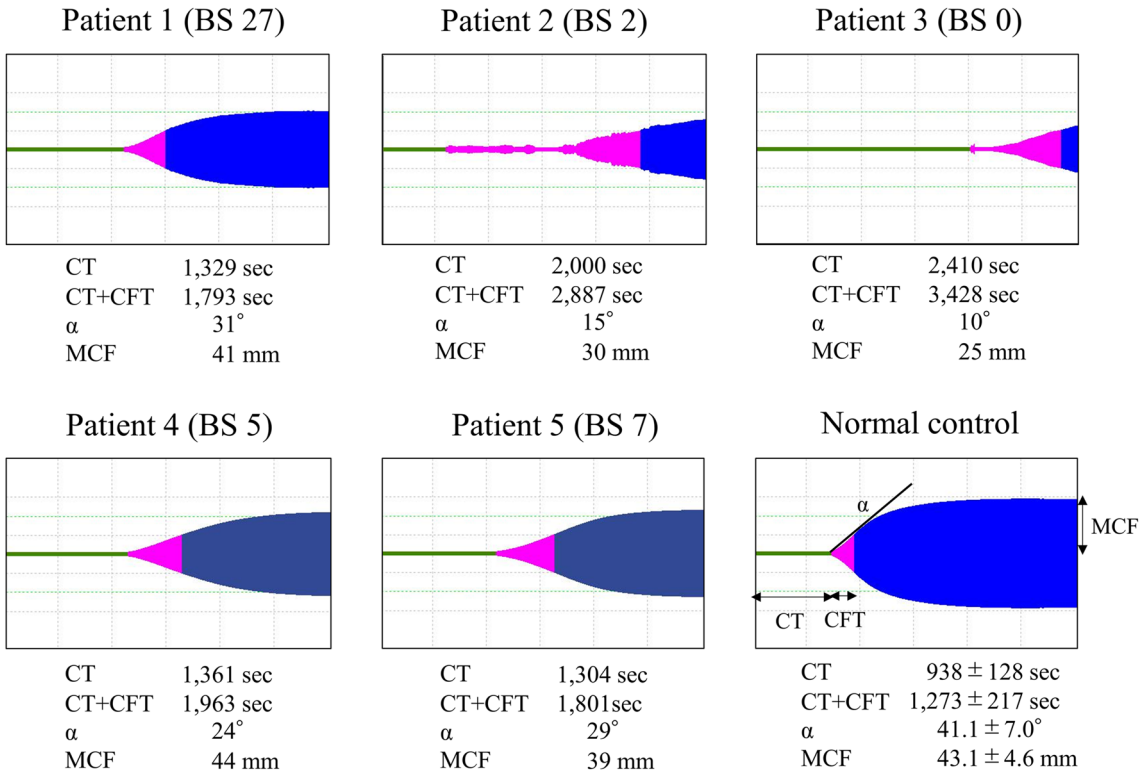

Fig. 1 ROTEM thromboelastograms in whole blood samples from type 2N VWD patients—$CaCl_2$ was added to each citrated whole blood sample from 5 patients with type 2N VWD for the ROTEM assay as described in Methods. ROTEM parameters (CT, CT + CFT, α-angle and MCF) are shown below each figure. CT, CT + CFT, α-angle and MCF obtained from normal controls ($n = 20$) were 938 ± 128 s, 1273 ± 217 s, 41.1 ± 7.0° and 43.1 ± 4.6 mm, respectively. *ROTEM* rotational thromboelastometry

in patients 2 and 3 were significantly lower (<−2SD), however, those in patients 1, 4 and 5 appeared to be close to normal range. These findings indicated that the ROTEM assays did not reflect the clinical severity in these type 2N VWD patients.

Correlation of T-TAS parameters with BS in type 2N VWD

We next investigated the relationship between BS and T-TAS parameters using collagen-coated PL-chips and collagen/thromboplastin-coated AR-chips.

PL-chip assay at high shear Representative pressure curves, images of PTF on the capillary surface and the T_{10} and AUC_{10} parameters are shown in Fig. 2a–c, respectively. In patient 1 (BS 27), the pressure curve in the PL assay was markedly depressed compared to control (Fig. 2a), and consequently the T_{10} was prolonged and AUC_{10} was markedly decreased relative to control (T_{10}; 4.1 ± 1.3 min, AUC_{10}; 265 ± 94 in 20 healthy controls) (Fig. 2c). Moreover, video microscopy confirmed only slight adhesion of platelets to the capillary surface at 4 min, and no subsequent growth of platelet aggregates, compared to the extensive PTF within a few minutes in normal whole blood (Fig. 2b). In contrast, in all other patients with various BS, the pressure curves and growth patterns of PTF were similar to normal control, and the T_{10} and AUC_{10} parameters in these 4 individuals were within the normal range.

AR-chip assay at low shear Representative pressure curves, images of fibrin-rich PTF on the capillary surface and AR-chip parameters (T_{10} and AUC_{30}) are shown in Fig. 3a–c, respectively. In patient 1, the video images showed no fibrin-rich PTF at 12 min (Fig. 3b), corresponding with a markedly delayed pressure curve (Fig. 3a). As with the PL assay in this patient, therefore, the T_{10} and AUC_{30} were severely abnormal. The T_{10} and AUC_{30} values in patients 4 (BS 5) and 5 (BS 7) were modestly abnormal, whilst these measurements in patients 2 (BS 2) and 3 (BS

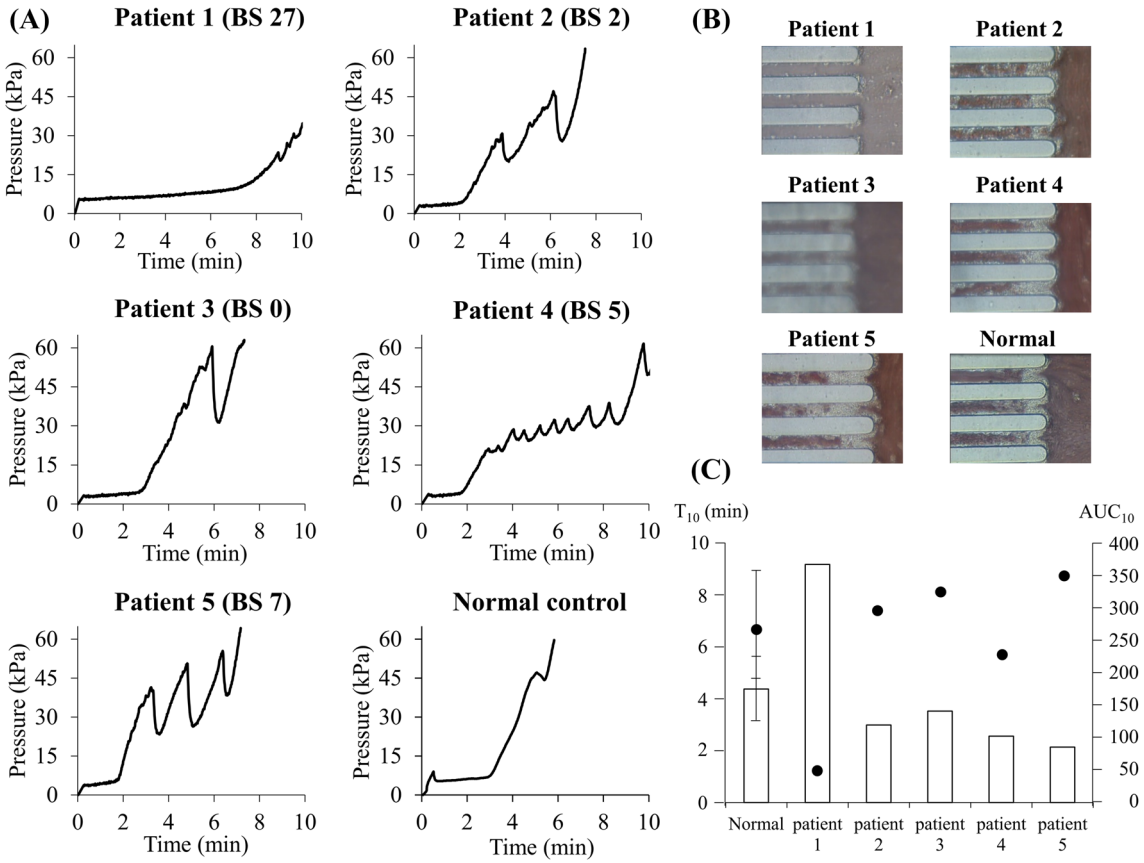

Fig. 2 T-TAS using the PL-chip in whole blood samples from type 2N VWD patients—**a** flow-pressure waveforms observed in whole blood from type 2N VWD patients and normal control individuals using the PL-chips in T-TAS. **b** The video-recorded images of PTF in whole blood from type 2N VWD patients at 4 min in the PL-chip are shown. **c** Whole blood samples from type 2N VWD patients were analyzed by the T-TAS at the shear rates of 1000 s^{-1} on the PL-chips. The T_{10} values in PL are shown as white bars, and area under the curve (AUC_{10}) in PL are shown as closed circles. Normal ranges are shown as the mean ± SD from 20 healthy controls (T_{10}; 4.1 ± 1.3 min, AUC_{10}; 265 ± 94)

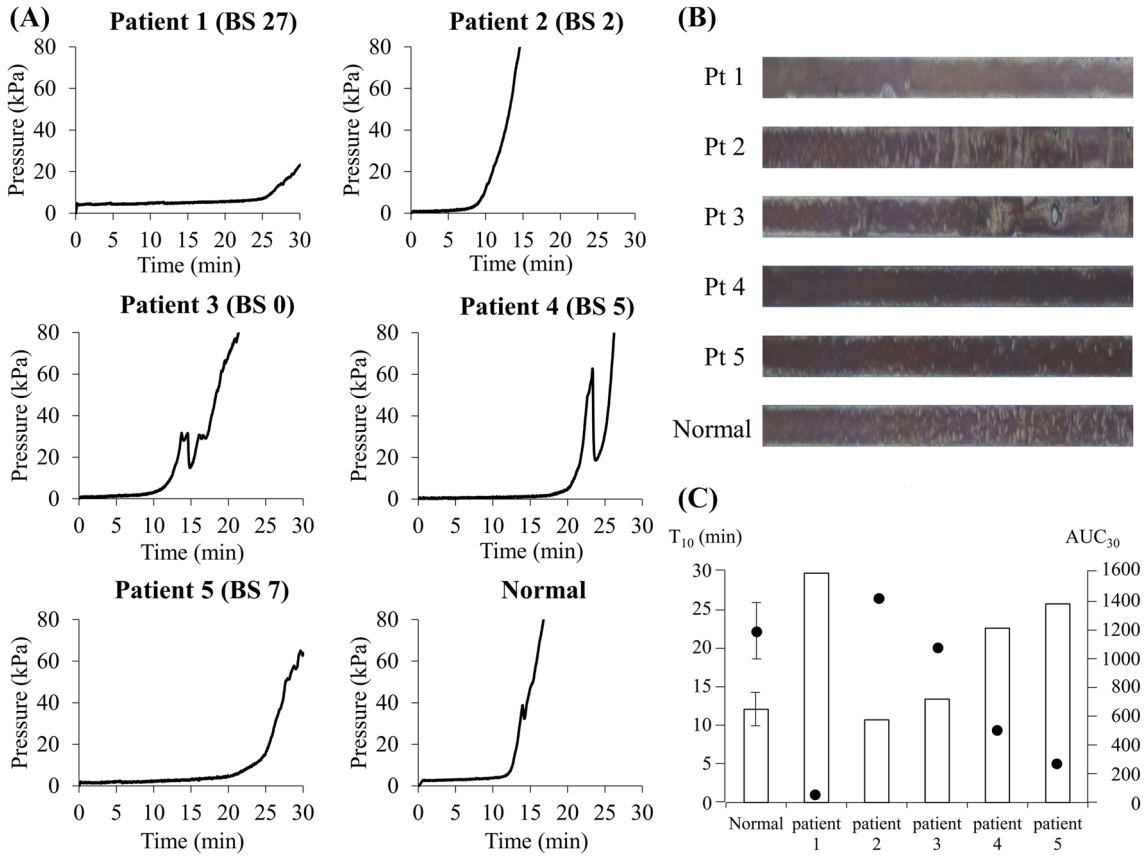

Fig. 3 T-TAS using the AR-chip in whole blood samples from type 2N patients—**a** flow-pressure waveforms observed in whole blood from type 2N VWD patients and normal control using AR-chips in T-TAS. **b** The video-recorded images of fibrin-rich PTF in whole blood from type 2N VWD patients at 12 min in the AR-chip are shown. *Pt* Patient. **c** Whole blood samples from type 2N VWD patients were analyzed by T-TAS at the shear rates of 240 s^{-1} on the AR-chips. The T_{10} values in AR are shown as white bars, and area under the curve (AUC_{30}) in AR are shown as closed circles. Normal ranges are shown as the mean ± SD from 20 healthy controls (T_{10}; 12.1 ± 2.1 min, AUC_{30}; 1221 ± 194)

0) were within the normal range (T_{10}; 12.1 ± 2.1 min, AUC_{30}; 1221 ± 194 in healthy controls) (Fig. 3c). In addition, the video images obtained in patients 1, 4 and 5 demonstrated a clear lack of fibrin-rich PTF at 12 min (Fig. 3b). A BS > 3 has been defined as representing an abnormal bleeding tendency [4, 23], and our findings indicated that both T_{10} and AUC_{30} correlated with the BS. The results suggested, therefore, that the AR-chip assay could be utilized to identify an abnormal bleeding tendency in the type 2N VWD patients.

In vivo effect of FVIII/VWF concentrates on thrombus formation

As described above, patient 1 had the highest BS and the most defective laboratory findings among our patients. She was treated successfully with the infusions of FVIII/VWF concentrates (30 IU/kg; calculated by FVIII:C) for severe gastrointestinal bleeding, and the effects of treatment were investigated using T-TAS. Figure 4 shows the pre- and post-infusion changes in the pressure curve (Fig. 4a), the T_{10} and AUC_{30} parameters (Fig. 4b) and the images of fibrin-rich PTF on the capillary surface (Fig. 4c). The results confirmed an improvement to normal in all of these analyses, and demonstrated that the T-TAS technique with the AR-chip could provide useful data for the assessment of therapy in type 2N VWD.

Discussion

The present study was designed to investigate laboratory assays to identify the clinical severity and measure the effects of therapy in patients with type 2N VWD. Viscoelastic hemostatic assays including ROTEM have been developed in recent years to provide rapid diagnostic information and guide appropriate therapeutic decisions in individual patients with a range of underlying coagulopathies. We have previously shown that comprehensive coagulation assays of

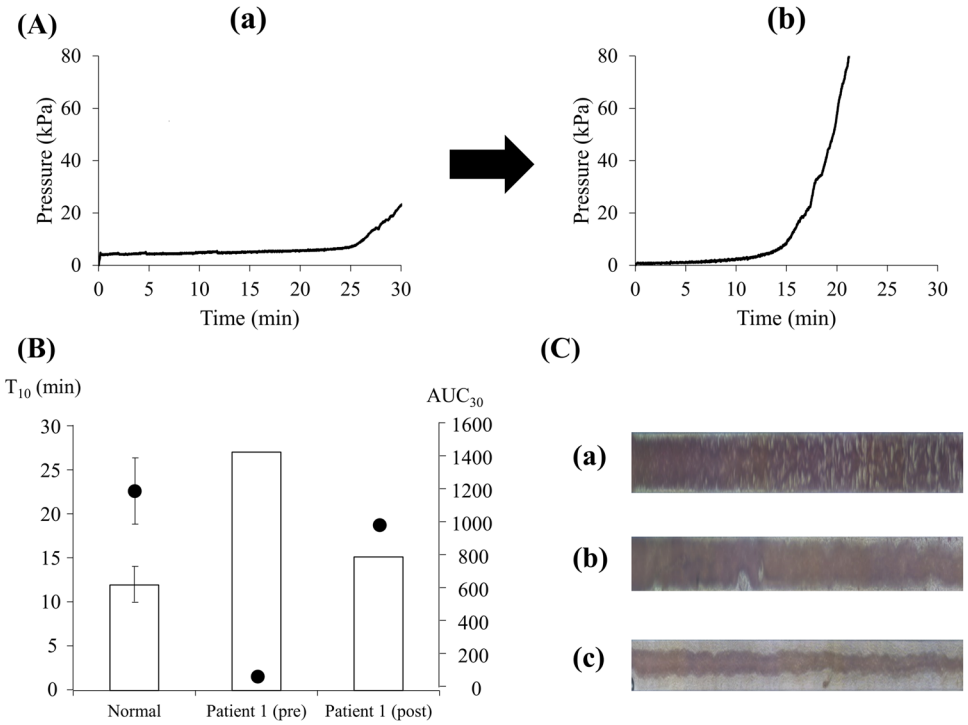

Fig. 4 In vivo effect of infusion of FVIII/VWF concentrates on T-TAS in type 2N VWD patient—**a** flow-pressure waveforms observed in whole blood samples before and after infusion of FVIII/VWF concentrates in patient 1 using the AR-chip in T-TAS. (a) Pre-infusion and (b) post-infusion. **b** Whole blood samples from patient 1 were analyzed by T-TAS at shear rates of 240 s^{-1} on the AR-chips. The T_{10} values in AR are shown as the white bars, and area under the curve (AUC_{30}) in AR is shown as closed circles. Normal ranges are shown as the mean ± SD from 20 healthy controls (see the Fig. 3). **c** The video-recorded images of fibrin-rich PTF in whole blood from patient 1 at 12 min. (a) Normal; (b) pre-infusion; (c) post-infusion of FVIII/VWF concentrates

this type may be useful for systematic monitoring of hemostatic management in hemophilia A patients with inhibition [22].

We have also demonstrated, however, that ROTEM analysis failed to discriminate between healthy subjects and various VWD patients [9], and our current investigations confirmed that ROTEM parameters did not reflect BS in type 2N VWD, but instead showed a differential diagnosis of mild hemophilia. Ågren et al. [11] also reported that the ROTEM parameters were within the normal range in type 3 VWD and were not affected by hemostatic therapy. It appeared evident, therefore, that ROTEM analysis did not reflect the clinical severity of VWD patients, and our present data confirmed that there was no correlation between ROTEM calculations and BS in type 2N VWD. In particular, it was interesting that the more pronounced defects were observed in patients 2 and 3 relative to patient 1 who featured a homozygous FVIII carrier defect and reduced VWF levels. This reason remains unclear. The shear stress forces induced in whole blood in ROTEM correspond to ~ 50 s^{-1}, and the principles of the technique appear to be focused on mechanisms of secondary hemostasis rather than on the primary hemostatic function. The relatively weak hemodynamic environment might not be sufficient enough to distinguish hemostatic potential in type 2N VWD patients with different BS.

Moreover, analysis of thrombus formation using T-TAS showed that collagen-coated PL-chips could not reliably identify an abnormal bleeding tendency in type 2N VWD. Significantly depressed thrombus formation was evident in patient 1 with this assay, but the results with the other patients were within the normal range. In general, the PL-chip is utilized to quantify platelet function [20], and patient 1 carried the *p*.R365X mutation previously reported in type 3 VWD primarily exhibiting primary hemostatic dysfunction. Ågren et al. also demonstrated that the AUC_{10} with the PL-chip was severely depressed in type 3 VWD even after treatment [11], and it seemed likely, therefore, that the PL-chip identified a similar abnormality in our patient 1. In addition, the PL-chip assay has been shown to be useful for type 1 VWD [10].

In contrast, our results using the collagen/thromboplastin-coated AR-chip successfully reflected clinical severity, and confirmed the therapeutic effects of infused FVIII/VWF concentrates. These findings were keeping in with previous studies demonstrating that the AR-chip assay mirrored the effectiveness of treatment in various types of VWD [9, 11]. Fressinaud et al. [24] have demonstrated that thrombus formation at both low shear rates (100 and 650 s^{-1}) was significantly decreased in severe hemophilia A patients, whereas no significant differences between severe hemophilia A patients and normal control were observed at high shear (2600 s^{-1}). Ogawa et al. [25] also reported that blood samples from FVIII-deficient mice showed normal thrombus growth in AR-chip under the shear rate of 1100 s^{-1} but exhibited significant decreased thrombus volume and height in the AR-chip at shear rate of 110 s^{-1}. Therefore, the AR-chip assay at low shear rate could reflect overall hemostatic functions mediated by

FVIII and VWF. The principal defect in type 2N VWD centers on the loss of VWF-binding potential to FVIII [26]. It seemed likely, therefore, that the flow-mediated VWF/FVIII function is important in the hemostasis of type 2N VWD and that AR-chip recognized the VWF/FVIII-binding defect, whilst the PL-chip did not. The photo images of AR-chip from whole blood samples in type 2N patients exhibited abnormal thrombus formation that had characteristics of a narrow and winding path of blood flow in the center of the capillary. The photo images of the post-infusion sample in type 2N patient similarly displayed the impaired thrombus patterns, despite improvements in AR-chip parameters. These results were consistent with our previous data [9], indicating that type 2N VWF proteins may still exist inside blood vessels and compete with normal VWF (FVIII/VWF concentrates).

Three VWF point mutations, *p*.E787K, *p*.T791M and *p*.R816W are known to be associated with the most severe clinical symptoms in type 2N VWD [27], and the *p*.R365X mutation has been identified as responsible for type 3 VWD [21]. Genetic analyses in the present study demonstrated that patient 1 had a compound heterozygous mutation (*p*.T791M/*p*.R365X) and patients 2–4 had heterozygous *p*.R816W. Van Meegeren et al. [23] reported that the median BS and VWF-related laboratory findings in genetically confirmed type 2N VWD patients were higher and lower those that in carriers, respectively. In our data, however, no significant difference was observed in laboratory results between type 2N VWD patient and heterozygous type 2N patients. Since we did not explore the whole VWF gene, patients 2–4 cannot be completely precluded to carry other VWF mutations. Thus, it may be that the discrepancy of laboratory results in patients 2–4 was due to other hemostatic defects in them. Nevertheless, the results indicated that genotyping provided a useful guide to clinical severity in type 2N VWD, and were consistent with the likelihood that the double genetic mutation in our patient 1 contributed to severe clinical symptoms.

Our current investigation was limited by the small number of patients available. The variability in T-TAS results as well as in BS may influence the results obtained in such a small number of patients. However, the findings further suggested that assessment of PTF, especially utilizing the collagen/thromboplastin-coated AR-chip in the commercially available automated microchip flow-chamber system, could provide a rapid means to predict the bleeding tendency and determine the hemostatic effects of therapy in type 2N VWD. A larger cohort study appears to be warranted to confirm the possibilities for improved laboratory analyses in these patients.

Acknowledgements We greatly thank Prof. Dr. Yoshiaki Tomiyama (Osaka University) and Dr. Hiroyuki Sugawara (Sumitomo Hospital) who was the patients' home doctor for keeping the patients' condition stable for a long term.

Author contributions YN: analyzed the data, made the figure, wrote the paper; KN: ran the clinic, performed the experiments, designed the research, interpreted the data, wrote the paper, edited the manuscript and approved the final version to be published, TK: analyzed VWF gene, KY, KO, SF, NS, MT: ran the clinic and performed the experiments; MS: supervised the research.

Funding This work was partly supported by a Grant-in-Aid for Scientific Research (KAKENHI) from the Ministry of Education, Culture, Sports, Science and Technology (MEXT) to KN (Grant No. 18K07885).

Compliance with ethical standards

Conflict of interest The authors have no conflicts of interest to disclose.

References

1. Sadler JE, Budde U, Eikenboom JC, Favaloro EJ, Hill FG, Holmberg L, et al. Update on the pathophysiology and classification of von Willebrand disease: a report of the Subcommittee on von Willebrand factor. J Thromb Haemost. 2006;4:2103–14.
2. Mazurier C, Goudemand J, Hilbert L, Caron C, Fressinaud E, Meyer D. Type 2N von Willebrand disease: clinical manifestations, pathophysiology, laboratory diagnosis and molecular biology. Best Pract Res Clin Haematol. 2001;14:337–47.
3. Dukka S, Allsup DJ. Perioperative management of type 2N Von Willebrand's disease with recombinant factor viii in a patient undergoing knee-replacement surgery. Case Rep Hematol. 2013;2013:837906.
4. de Wee EM, Sanders YV, Mauser-Bunschoten EP, van der Bom JG, Degenaar-Dujardin ME, Eikenboom J, et al. Determinants of bleeding phenotype in adult patients with moderate or severe von Willebrand disease. Thromb Haemost. 2012;108:683–92.
5. Rydz N, James PD. The evolution and value of bleeding assessment tools. J Thromb Haemost. 2012;10:2223–9.
6. Tosetto A, Rodeghiero F, Castaman G, Goodeve A, Federici AB, Batlle J, et al. A quantitative analysis of bleeding symptoms in type 1 von Willebrand disease: results from a multicenter European study (MCMDM-1 VWD). J Thromb Haemost. 2006;4:766–73.
7. Tsuji S, Sugimoto M, Miyata S, Kuwahara M, Kinoshita S, Yoshioka A. Real-time analysis of mural thrombus formation in various platelet aggregation disorders: distinct shear-dependent roles of platelet receptors and adhesive proteins under flow. Blood. 1999;94:968–75.
8. Sugimoto M, Matsui H, Mizuno T, Tsuji S, Miyata S, Matsumoto M, et al. Mural thrombus generation in type 2A and 2B von Willebrand disease under flow conditions. Blood. 2003;101:915–20.
9. Ogiwara K, Nogami K, Hosokawa K, Ohnishi T, Matsumoto T, Shima M. Comprehensive evaluation of haemostatic function in von Willebrand disease patients using a microchip-based flow chamber system. Haemophilia. 2015;21:71–80.
10. Nogami K, Ogiwara K, Yada K, Shida Y, Takeyama M, Yaoi H, et al. Assessing the clinical severity of type 1 von WIllebrand disease patients with a microchip flow-chamber system. J Thromb Haemost. 2016;14:667–74.

11. Ågren A, Holmström M, Schmidt DE, Hosokawa K, Blombäck M, Hjemdahl P. Monitoring of coagulation factor therapy in patients with von Willebrand disease type 3 using a microchip flow chamber system. Thromb Haemost. 2017;117:75–85.
12. Nishino M, Nishino S, Sugimoto M, Shibata M, Tsuji S, Yoshioka A. Changes in factor VIII binding capacity of von Willebrand factor and factor VIII coagulant activity in two patients with type 2N von Willebrand disease after hemostatic treatment and during pregnancy. Int J Hematol. 1996;64:127–34.
13. Shibata M, Shima M, Fujimura Y, Takahashi Y, Nakai H, Sakurai Y, et al. Identification of the binding site for an alloantibody to von Willebrand factor which inhibits binding to glycoprotein Ib within the amino-terminal region flanking the A1 domain. Thromb Haemost. 1999;81:793–8.
14. Macfarlane DE, Stibbe J, Kirby EP, Zucker MB, Grant RA, McPherson J. A method for assaying von Willebrand factor (ristocetin cofactor). Thromb Diath Haemorrh. 1975;34:306–8.
15. Duncan E, Rodgers S. One-stage factor VIII Assays. Methods Mol Biol. 2017;1646:247–63.
16. Fujimura Y, Usami Y, Titani K, Niinomi K, Nishio K, Takase T, et al. Studies on anti-von Willebrand factor (vWF) monoclonal antibody NMC-4, which inhibits both ristocetin- and botrocetin-induced vWF binding to platelet glycoprotein Ib. Blood. 1991;77:113–20.
17. Yada K, Nogami K, Takeyama M, Ogiwara K, Wakabayashi H, Shima M. Mild hemophilia A patient with novel Pro1809Leu mutation develops an anti-C2 antibody inhibiting allogeneic but not autologous factor VIII activity. J Thromb Haemost. 2015;13:1843–53.
18. James PD, Notley C, Hegadorn C, Leggo J, Tuttle A, Tinlin S, et al. The mutational spectrum of type 1 von Willebrand disease: results from a Canadian cohort study. Blood. 2007;109:145–54.
19. Bowman M, Lillicrap D, James P. The genetics of Canadian type 3 von Willebrand disease: further evidence for codominant inheritance of mutant alleles: a reply to a rebuttal. J Thromb Haemost. 2013;11:1786–7.
20. Hosokawa K, Ohnishi T, Kondo T, Furukawa M, Koide T, Maruyama I, et al. A novel automated microchip flow-chamber system to quantitatively evaluate thrombus formation and antithrombotic agents under blood flow conditions. J Thromb Haemost. 2011;9:2029–37.
21. Baronciani L, Cozzi G, Canciani MT, Peyvandi F, Srivastava A, Federici AB, et al. Molecular defects in type 3 von Willebrand disease: updated results from 40 multiethnic patients. Blood Cells Mol Dis. 2003;30:264–70.
22. Furukawa S, Nogami K, Ogiwara K, Yada K, Minami H, Shima M. Systematic monitoring of hemostatic management in hemophilia A patients with inhibitor in the perioperative period using rotational thromboelastometry. J Thromb Haemost. 2015;13:1279–84.
23. van Meegeren ME, Mancini TL, Schoormans SC, van Haren BJ, van Duren C, Diekstra A, et al. Clinical phenotype in genetically confirmed von Willebrand disease type 2N patients reflects a haemophilia A phenotype. Haemophilia. 2015;21:375–83.
24. Fressinaud E, Sakariassen KS, Rothschild C, Baumgartner HR, Meyer D. Shear rate-dependent impairment of thrombus growth on collagen in nonanticoagulated blood from patients with von Willebrand disease and haemophilia. Blood. 1992;80:988–94.
25. Ogawa S, Szlam F, Dunn AL, Bolliger D, Ohnishi T, Hosokawa K, et al. Evaluation of a novel flow chamber system to assess clot formation in factor FVIII-deficient mouse and anti-factor IXa-treated human blood. Haemophilia. 2012;18:926–32.
26. Castaman G, Goodeve A, Eikenboom J. Principles of care for the diagnosis and treatment of von Willebrand disease. Haematologica. 2013;98:667–74.
27. Hampshire DJ, Goodeve AC. The international society on thrombosis and haematosis von Willebrand disease database: an update. Semin Thromb Hemost. 2011;37:470–9.